PSFC/JA-05-18

Current Drive by Electron Bernstein Waves in Spherical Tori

A. K. Ram, J. Decker,
G. Taylor, [a] P. C. Efthimion, [a]
C. N. Lashmore-Davies, [b] R. A. Cairns [c]

August 2005

Plasma Science and Fusion Center, Massachusetts Institute of Technology
Cambridge, MA 02139 U.S.A.

[a] Princeton Plasma Physics Laboratory
Princeton, NJ 08543 U.S.A.

[b] Culham Science Centre, United Kingdom Atomic Energy Authority (UKAEA)
Abingdon, Oxon OX14 3DB United Kingdom

[c] University of St. Andrews
Fife KY16 9SS Scotland

This work was supported by the U.S. Department of Energy, Grant No. DE-FG02-91ER-54109, by the U.S. Department of Energy jointly with the National Spherical Torus Experiment, Grant No. DE-FG02-99ER-54521, UK EPSRC, and EURATOM.

To appear in *Proceedings of the 20th International Atomic Energy Agency (IAEA) Fusion Energy Conference,* Vilamoura, Portugal, November 1–6, 2004.

Current Drive By Electron Bernstein Waves in Spherical Tori

A.K. Ram 1), J. Decker 1), G. Taylor 2), P.C. Efthimion 2), C.N. Lashmore-Davies 3), R.A. Cairns 4)

1) Plasma Science & Fusion Center, M.I.T., Cambridge, MA, 02139, U.S.A.
2) Princeton Plasma Physics Laboratory, Princeton, NJ , 08543, U.S.A.
3) EURATOM/UKAEA Fusion Association, Culham Science Centre, Abingdon, Oxon, OX14 3DB, U.K.
4) University of St. Andrews, St. Andrews, Fife, KY16 9SS U. K.

e-mail contact of main author abhay@psfc.mit.edu

Abstract. The high-β operating regime of spherical tokamaks (ST), such as in NSTX and MAST, make them attractive fusion devices. For access to such high β regimes, it is necessary to heat and to drive currents in ST plasmas. While such plasmas are overdense to conventional electron cyclotron waves, electron Bernstein waves (EBW) offer an attractive means toward this purpose. The applications of EBWs in STs range from plasma start-up and heating of the ST plasma to modifying and controlling its current profile. The controlling of the current profile could provide better confinement as well as help suppress neoclassical tearing modes. This paper deals with two particular topics. The first topic is on the relevance of relativistic effects in describing the propagation and damping of EBWs. The second topic is on plasma current generation by EBWs.

1. Introduction

In order to achieve the high βs, STs generally operate at low magnetic fields and high densities such that $\omega_p/\omega_c >> 1$ over most of the plasma. Here ω_p and ω_c are the angular electron plasma and cyclotron frequencies, respectively. Such an overdense nature of ST plasmas makes them unsuitable for heating and/or current drive by the conventional ordinary O and extraordinary X modes in the electron cyclotron (EC) range of frequencies. For low harmonics of ω_c the X and O modes are cutoff near the edge of the plasma. For high harmonics these modes do access the core of the ST plasma but are essentially undamped when they encounter the electron cyclotron resonances. However, EBWs offer an attractive alternative in the EC frequency range as

they have no density cutoffs, and damp strongly on electrons at the fundamental, or any harmonic of the Doppler-shifted electron cyclotron resonance [1]. Since EBWs cannot propagate in vacuum (like the X and O modes) they are excited, indirectly, by mode conversion of externally launched O mode or X mode [1, 2, 3, 4]. In this paper we do not discuss the mode conversion excitation of EBWs as it has already been covered in the literature.

In studying the propagation and damping of the traditional X and O modes in the EC frequency range it has been noted that weakly relativistic effects are important [5, 6]. We find that for EBWs the same, weakly relativistic, formalism for the wave description cannot be used. Also, for EBWs, unlike the X and O modes, $k_\perp \rho_e$ can easily exceed 1 as the waves propagate away from the mode conversion region into the plasma core [1]. ($k_\perp$ is the wave vector perpendicular to the magnetic field and ρ_e is the electron Larmor radius.) Thus, we cannot do any Larmor radius expansions of the dielectric tensor elements. Consequently, we have developed a code R2D2 which solves the fully relativistic wave dispersion relation. Our initial results from R2D2 indicate that relativistic effects are important for EBWs in a ST plasma away from the mode conversion edge region.

An important role for EBWs in STs could be to generate non-inductive plasma currents. A study of the propagation of EBWs in a toroidal equilibrium using a non-relativistic ray trajectory code shows that the parallel wave number $n_\parallel = ck_\parallel/\omega$ can change from well below 1 to above 1 along the ray path [1]. ($k_\parallel$ is the component of the wave vector parallel to the magnetic field, c is the speed of light, and ω is the wave angular frequency.) This is primarily due to the poloidal magnetic field. Consequently, the accessible phase space for current drive by EBWs is richer than for the X and O modes. For the X and O modes the resonance surfaces for the wave-electron interactions are elliptic while the diffusion paths lie along hyperbolas. The EBWs not only have these properties for $n_\parallel < 1$, but also the property that the resonance surfaces become hyperbolic and the diffusion paths become elliptic for $n_\parallel > 1$. A drift kinetic Fokker-Planck code DKE [7] which includes a quasilinear RF diffusion operator and the effect of trapped electrons is being used to study EBW current drive. Preliminary results show that in the outer half of a ST plasma, where trapped electron population is significant, EBWs effectively drive current through the Ohkawa mechanism [8, 9]. In the core of the plasma where the fraction of trapped electrons is reduced, EBWs effectively generate current through the Fisch-Boozer scheme [10].

2. Relativistic Propagation of Electron Bernstein Waves

We follow Trubnikov's formalism for the derivation of the relativistic dielectric tensor [11]. From the linearized Vlasov equation, the perturbed distribution function is

$$f_1 = \; - \; \frac{1}{\Omega} \exp\left\{ \frac{-i}{\Omega} \left(\lambda\phi - \frac{p_\perp k_\perp}{m\gamma} \sin\left(\phi - \psi\right) \right) \right\} \times \int_{-\infty}^{\phi} d\phi' \exp\left\{ \frac{i}{\Omega} \left(\lambda\phi' - \frac{p_\perp k_\perp}{m\gamma} \sin\left(\phi' - \psi\right) \right) \right\} \hat{P}' \; f_0\left(p_\perp, p_\parallel\right) \quad (1)$$

where f_0 is the unperturbed distribution function for the electrons,

$$\frac{\hat{P}}{-q} = \frac{1}{\sqrt{2}} \left(E_l e^{-i\phi} + E_r e^{i\phi} \right) \hat{G} + E_\parallel \left(\frac{k_\perp}{\omega} \cos\left(\psi - \phi\right) \hat{H} + \frac{\partial}{\partial p_\parallel} \right) \quad (2)$$

$$\hat{G} = \frac{\partial}{\partial p_\perp} - \frac{k_\parallel}{\omega} \hat{H}, \qquad \hat{H} = \frac{p_\parallel}{m\gamma} \frac{\partial}{\partial p_\perp} - \frac{p_\perp}{m\gamma} \frac{\partial}{\partial p_\parallel} \quad (3)$$

$$\lambda = \omega - \frac{k_\parallel p_\parallel}{m\gamma}, \quad \gamma = \left(1 + \frac{p_\perp^2}{m^2c^2} + \frac{p_\parallel^2}{m^2c^2} \right)^{1/2}, \quad \Omega = \frac{qB_0}{m\gamma}, \quad (4)$$

$$p_x = p_\perp \cos\left(\phi\right), \quad k_x = k_\perp \cos\left(\psi\right), \quad \sqrt{2} E_{l,r} = E_x \pm i E_y. \quad (5)$$

The plasma conductivity tensor is obtained from the current density

$$\vec{j} \; = \; q \int \; d^3p \; \frac{\vec{p}}{m\gamma} \left(f_0 + f_1 \right) \; = \; \overline{\overline{\sigma}} \cdot \vec{E} \quad (6)$$

There are two complementary approaches for obtaining $\overline{\overline{\sigma}}$ [11]. The first is to perform the momenta integrals analytically and do the ϕ' (time history) integral in (1) numerically. This essentially works for a relativistic Maxwellian $f_0(p_\perp, p_\parallel)$. The second technique, is to perform the ϕ' (time history) integral analytically and do the momenta integrals in (6) numerically. This technique is valid for arbitray f_0's.

For a relativistic Maxwellian the first approach leads to the following form of the conductivity tensor:

$$\overline{\overline{\sigma}} = \frac{1}{4\pi} \frac{\omega_p^2}{\omega_c} \; \frac{c^4}{v_t^4} \frac{1}{\mathrm{K}_2\left(\dfrac{c^2}{v_t^2} \right)} \; \int_0^\infty d\xi \quad \left\{ \frac{\mathrm{K}_2\left(R^{1/2}\right)}{R} \overline{\overline{T}}_1 - \frac{\mathrm{K}_3\left(R^{1/2}\right)}{R^{3/2}} \; \overline{\overline{T}}_2 \right\} \quad (7)$$

where ω_p, ω_c, v_t are the rest mass electron plasma frequency, cyclotron frequency, and the thermal velocity, respectively, K_ν is the modified Bessel function of the second kind of order ν,

$$\overline{\overline{T}}_1 = \begin{pmatrix} \cos\xi & -\sin\xi & 0 \\ \sin\xi & \cos\xi & 0 \\ 0 & 0 & 1 \end{pmatrix} \tag{8}$$

$$\overline{\overline{T}}_2 = \frac{c^2}{\omega_c^2} \begin{pmatrix} k_\perp^2 \sin^2\xi & -k_\perp^2 \sin\xi\,(1-\cos\xi) & k_\perp k_\parallel \xi \sin\xi \\ k_\perp^2 \sin\xi\,(1-\cos\xi) & -k_\perp^2\,(1-\cos\xi)^2 & k_\perp k_\parallel \xi\,(1-\cos\xi) \\ k_\perp k_\parallel \xi \sin\xi & -k_\perp k_\parallel \xi\,(1-\cos\xi) & k_\parallel^2 \xi^2 \end{pmatrix} \tag{9}$$

$$R = \left(\frac{c^2}{v_t^2} - i\xi\frac{\omega}{\omega_c}\right)^2 + 2\left(\frac{k_\perp c}{\omega_c}\right)^2 (1-\cos\xi) + \frac{k_\parallel^2 c^2 \xi^2}{{\omega_c}^2} \tag{10}$$

For any equilibrium distribution function $f_0(p_\perp, p_\parallel)$ the second approach leads to the following conductivity tensor:

$$\overline{\overline{\sigma}} = -\frac{i}{2}\,\frac{\omega_p^2}{\omega_c} \left\langle \sum_{n=-\infty}^{\infty} \frac{1}{n-\overline{\omega}} \left(\frac{1}{\kappa T}\,\frac{p_\perp}{m\gamma}\right) \overline{\overline{\sigma}}_N\; f_0\left(p_\perp, p_\parallel\right) \right\rangle \tag{11}$$

where

$$\overline{\overline{\sigma}}_N = \begin{pmatrix} \frac{n^2}{\zeta^2} p_\perp \mathrm{J}_n^2 & -i\frac{n}{\zeta} p_\perp \mathrm{J}_n \mathrm{J}_n' & \frac{n}{\zeta} p_\parallel \mathrm{J}_n^2 \\ i\frac{n}{\zeta} p_\perp \mathrm{J}_n \mathrm{J}_n' & p_\perp \mathrm{J}_n'^2 & i p_\parallel \mathrm{J}_n \mathrm{J}_n' \\ \frac{n}{\zeta} p_\parallel \mathrm{J}_n^2 & -i p_\parallel \mathrm{J}_n \mathrm{J}_n' & \frac{p_\parallel^2}{p_\perp} \mathrm{J}_n^2 \end{pmatrix} \tag{12}$$

$$\zeta = \frac{k_\perp p_\perp}{m\omega_c}, \overline{\omega} = \frac{1}{\omega_c}\left(\omega\gamma - k_\parallel \frac{p_\parallel}{m}\right), \omega_c = \frac{eB_0}{m}, \langle ..... \rangle = \int_0^\infty dp_\perp p_\perp \int_{-\infty}^\infty dp_\parallel \tag{13}$$

We have developed two separate numerical routines within the code R2D2 which are based on the two relativistic formalisms discussed above. For a variety of cases we find that the two formalisms lead to numerically identical results. Since we are not aware of any similar code in existence, this allows us to benchmark our code. In Fig. 1 we compare the results obtained from the relativistic description (red) with those obtained from the non-relativistic

description (blue) in the mode conversion region for NSTX model equilibrium [1]. We find that there is essentially no difference between the two cases in the low temperature region where the mode coupling takes place. Thus, the mode conversion formalism developed in [1, 2, 3, 4] is not modified by relativistic effects. However, the EBW part of the dispersion relation begins to show some differences away from the mode conversion region. In Fig. 2 we show the dispersion characteristics of EBWs as a function of $n_\parallel$ for a uniform plasma with electron temperature of 3 keV, $\omega_p/\omega_c = 6$, and $\omega/\omega_c = 1.8$. It is now evident that there are significant differences between the relativistic and non-relativistic properties of EBWs. This could have important consequences when studying the propagation and damping of EBWs in ST plasmas.

3. Electron Bernstein Waves Current Drive

As part of the overall scheme to use EBWs for driving plasma currents in a ST, and possibly for achieving a steady-state operation, it is important to understand the parametric dependence of EBW current drive efficiency. The relativistic code DKE [7] is being used for studying the EBW driven current. This code solves in two-dimensional momentum space, on a given flux surface, the neoclassical drift-kinetic equation with a RF quasilinear diffusion operator. In deriving the equations solved in DKE, we assume that the electron guiding center drift velocity across the flux surfaces is small compared to its streaming velocity along the field line. We further assume weak collisionality so that the banana approximation is valid. This implies that the bounce time of trapped electrons is much shorter than the collisional detrapping time. The bounce time is also assumed to be shorter than the RF induced diffusion time. Consequently, the electron distribution function is uniform along the field lines. To leading order in the small parameter defined by the ratio of the bounce time to the drift time, the electron distribution function $f(p_\perp, p_\parallel)$ in momentum space is obtained from the bounce averaged Fokker-Planck equation $\langle C(f) + Q(f) \rangle$, where C is the collision operator and Q is the quasilinear diffusion operator. DKE is used to solve this Fokker-Planck equation for $f(p_\perp, p_\parallel)$. The quasilinear diffusion coefficient $Q(f)$ in DKE is determined from R2D2. By taking the appropriate moments of f we can solve for the parallel current and the power dissipated and, consequently, evaluate the current drive efficiency $\eta = (J/en_e v_{te})/(P/\nu_e m_e n_e v_{te}^2)$. Here J is the current density, P is the density of power dissipated, e is the electron charge, m_e is the electron mass, n_e,v_{te}, and ν_e are the local electron density,

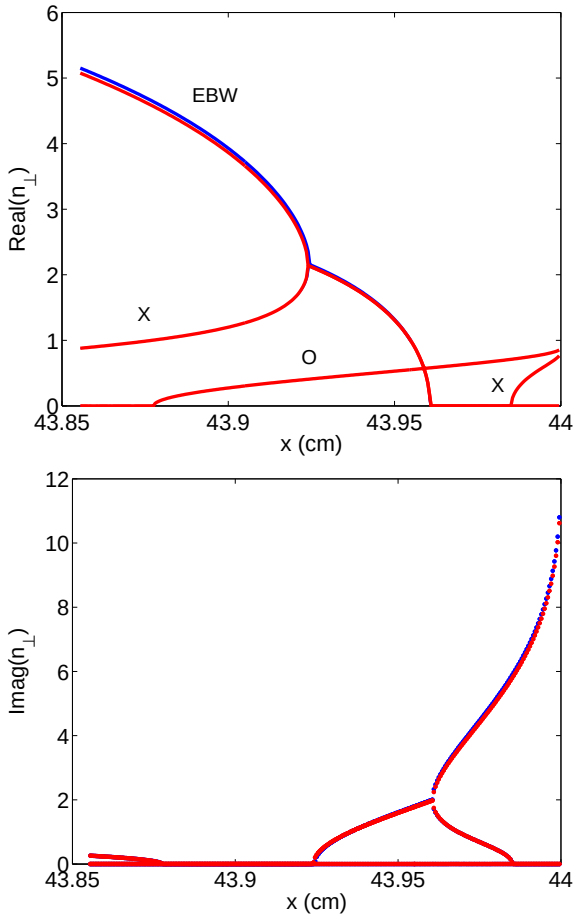

Figure 1: Real (left) and imaginary (right) part of $n_\perp = ck_\perp/\omega$ versus distance on the equatorial plane for NSTX-type parameters [1]. The comparison is between the relativistic (red) and non-relativistic (blue) characteristics of ECRF waves in the mode conversion region.

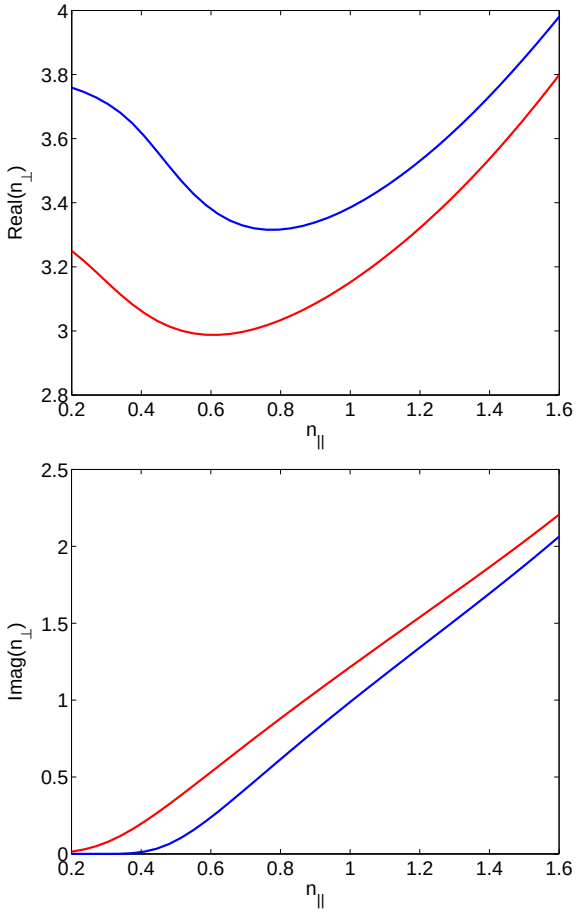

Figure 2: Real (left) and imaginary (right) part of $n_\perp$ versus $n_\parallel$. The comparison is between the relativistic (red) and non-relativistic (blue) characteristics of EBWs.

thermal velocity, and collision frequency, respectively. In our initial studies described below, we use the non-relativistic form of the EBW diffusion coefficient in $Q(f)$. The non-relativistic evaluation takes substantially less time than the relativistic calculation.

As an example of EBW current drive, we consider a NSTX-type plasma with major radius of 0.9 m, minor radius of 0.6 m, on axis magnetic field of 0.35 T, plasma current of 0.8 MA, peak electron temperature of 3 keV, and a peak electron density of 3×10^{19} m^{-3}. The density and temperature profiles are assumed to be parabolic. In this high β regime, the poloidal field is comparable to the toroidal field on the outboard part of the plasma. We assume an EBW wave frequency of $\omega/2\pi = 11.8$ GHz and $n_{\|} = 1.5$. We also consider a single EBW ray propagating along the equatorial plane with an input power in the ray of 1 MW. The left panel of Fig. 3 shows that the wave frequency matches the Doppler-shifted (second harmonic) electron cyclotron frequency where the total magnetic field is a minimum. The results from DKE are plotted in the right panel of Fig. 3. The peak current density is $J_{\rm peak} \approx 0.64$ MA m^{-2}. At this location the density of power dissipated is $P_{\rm peak} \approx 1.4$ MW m^{-3}. This leads to $\eta_{\rm peak} \approx 3.2$. This current drive efficiency is significantly higher than is generally achieved by conventional ECRF waves in tokamaks. From the left panel of Fig. 3 the location where the EBW frequency matches the Doppler-shifted cyclotron resonance occurs where the magnetic field is nearly flat (red line tangent to the green line). This leads to a large optical depth and the EBW interacts with energetic electrons in the distribution function. Consequently, we also obtain high current drive efficiencies. This shows that the non-monotonic magnetic field profile has important implications for EBW current drive in STs. The left panel of Fig. 4 shows that the phase velocity of the waves is in a direction opposite to the direction of the driven current. The region of maximum diffusion is situated near the trapped/passing boundary leading to a large EBW-induced trapping of passing electrons. The right panel illustrates this more clearly. The depletion of electrons due to trapping induced by EBWs in the region where the wave-particle resonance exists, and the accumulation of electrons due to detrapping on the opposite side (in $p_{\|}$) contribute to the current. This indicates that the current driven is the Ohkawa current [8, 9] rather than the Fisch-Boozer current [10]. Recent numerical simulations [12] have shown similar results.

Figure 5 corresponds to Fig. 3 for a wave frequency of 19.5 GHz and $n_{\|} = 0.5$. The peak current density is $J_{\rm peak} \approx 2.6$ MA m^{-2}. At this loca-

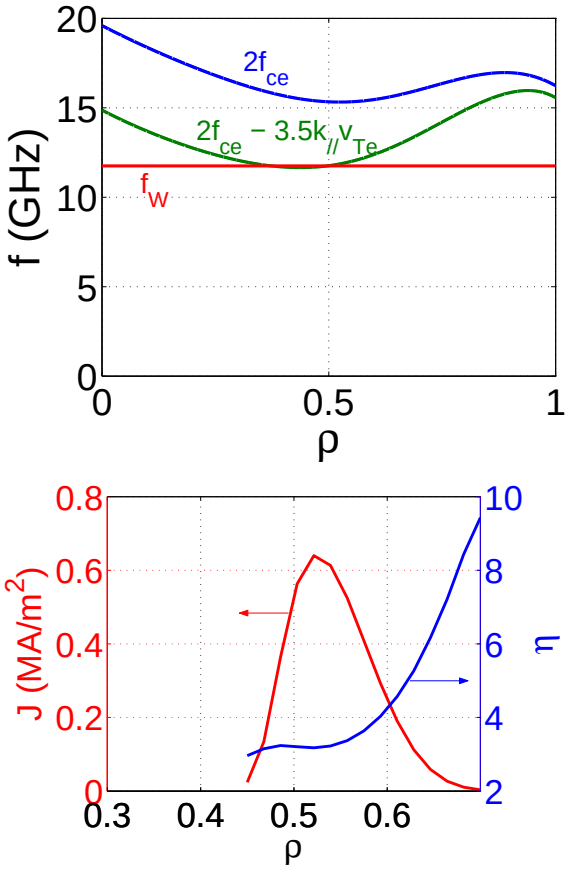

Figure 3: Left: wave frequency (f_w), second harmonic of the electron cyclotron frequency ($2f_{ce}$), and the Doppler-shifted (second harmonic) electron cyclotron frequency (in green) as a function of ρ (radial distance normalized to the minor radius); right: current density (red) and efficiency (blue) as a function of ρ.

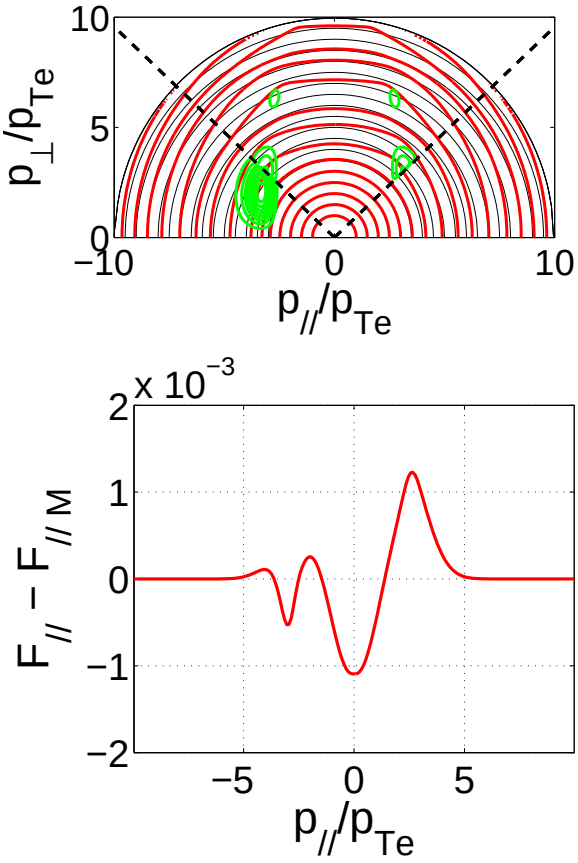

Figure 4: Left: contours of Maxwellian distribution (black) and distribution function (red) in the presence of EBW diffusion coefficient (contours in green); right: the parallel component of the RF driven distribution function, with the Maxwellian contribution subtracted off, as a function of the parallel momentum normalized to the thermal momentum.

tion the density of power dissipated is $P_{\rm peak} \approx 6.1$ MW m^{-3}. This leads to $\eta_{\rm peak} \approx 1.9$. From the two panels in Fig. 6 we note that this is the conventional Fisch-Boozer scheme of current drive. The EBW induced diffusion of electrons changes the resistivity non-symmetrically (in $p_\parallel$) leading to the current generation. However, the trapping effects reduce the current drive efficiency. Studies are underway to determine the conditions for optimizing the Fisch-Boozer current drive and the Ohkawa current drive schemes in an ST.

In conclusion, our calculations show that relativistic effects are important in describing the propagation and damping of EBWs in ST plasmas. Furthermore, our calculations on EBW current drive show that the Ohkawa current drive is more suitable for the outer half of the plasma while the Fisch-Boozer current drive works well near the core. Thus, the EBW spectrum could be tailored, according to the needs, for current generation and current profile control. Detailed studies on relativistic effects in EBW propagation and damping, and on the EBW driven current are continuing. Along with the previous results on coupling and excitation of EBWs the results from these studies will provide a general basis for defining the role of EBWs in present-day experiments and future ST power plants.

This work was supported by DOE Grant Numbers DE-FG02-91ER-54109 and DE-FG02-99ER-54521, and by UK EPSRC, and EURATOM.

References

[1] A. K. Ram and S. D. Schultz, *Phys. Plasmas* **7**, 4084 (2000).

[2] J. Preinhaelter and V. Kopecky, *J. Plas. Phys.* **10**, 1 (1973).

[3] A. K. Ram and A. Bers, *Nucl. Fus.* **43**, 1305 (2003).

[4] A. K. Ram, A. Bers, and C. N. Lashmore-Davies, *Phys. Plasmas* **9**, 409 (2002).

[5] G. LeClair, I.P. Shkarofsky, Y. Demers, and J-F. Mercier, in *Proc. 12th Topical Conf. on RF Power in Plasmas,* A.I.P. Conf. Proc. 403 (eds. P. M. Ryan and T. Intrator), Woodbury, New York (1997), p. 219.

[6] M. Bornatici, R. Cano, O. De Barbieri, and F. Engelmann, *Nuclear Fusion* **23**, 1153 (1983).

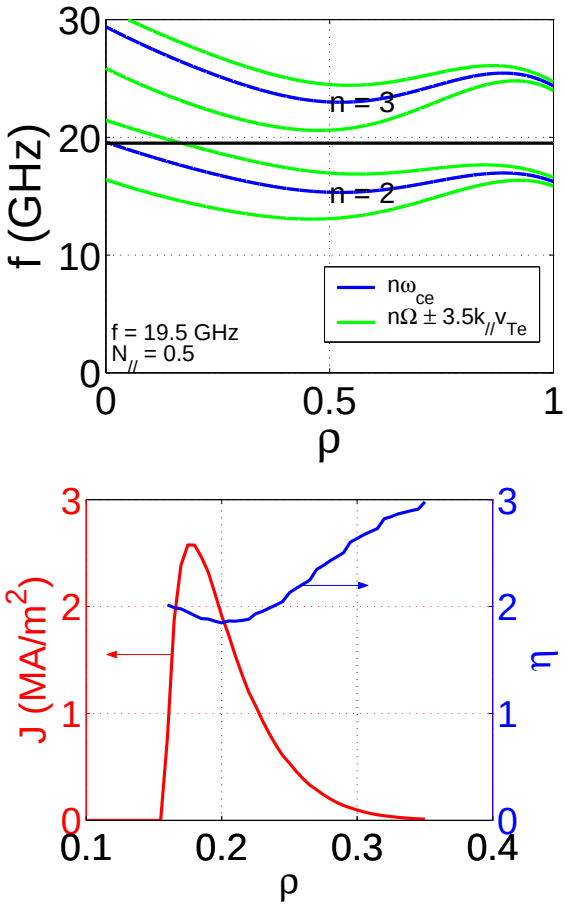

Figure 5: Left: wave frequency (f_w), second ($2f_{ce}$) and third ($3f_{ce}$) harmonic of the electron cyclotron frequency, and the corresponding Doppler-shifted electron cyclotron frequencies (in green) as a function of ρ; right: current density (red) and efficiency (blue) as a function of ρ.

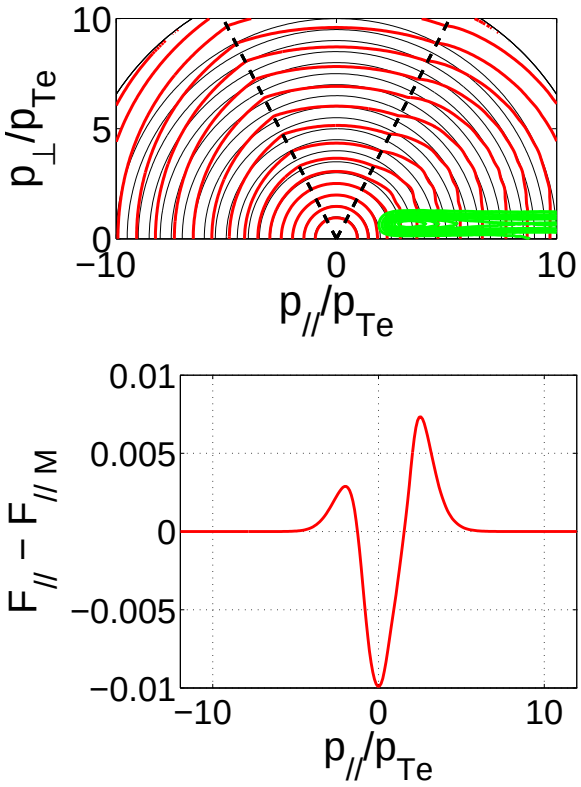

Figure 6: left: contours of Maxwellian distribution (black) and distribution function (red) in the presence of EBW diffusion coefficient (contours in green); right: parallel component of the RF driven distribution function, with the Maxwellian contribution subtracted off, versus $p_{\|}/p_{Te}$. .

[7] Y. Peysson, J. Decker, and R.W. Harvey, in *Proc. 15th Topical Conf. on RF Power in Plasmas*, AIP Conf. Proc. No. 694 (ed. C.B. Forest), Melville, New York (2003), p. 495.

[8] T. Ohkawa, General Atomics Report No. GA-A13847 (1976).

[9] More recently Ohkawa current drive using waves in the electron cyclotron range of frequencies has been discussed by: J. Decker, in *Proc. 15th Topical Conf. on RF Power in Plasmas*, AIP Conf. Proc. No. 694 (ed. C.B. Forest), Melville, New York (2003), p. 447.

[10] N.J. Fisch and A. Boozer, *Phys. Rev. Lett.* **45**, 720 (1980).

[11] B. A. Trubnikov, in *Plasma Physics and the Problem of Controlled Thermonuclear Reaction*, edited by M. A. Leontovich (Pergamon Press, New York, 1959), Vol. III.

[12] G. Taylor et al., *Phys. Plasmas* **11**, 4733 (2004).